frontiers in Marine Science

ORIGINAL RESEARCH
published: 07 January 2022
doi: 10.3389/fmars.2021.789687

Shelf Transport Pathways Adjacent to the East Australian Current Reveal Sources of Productivity for Coastal Reefs

Moninya Roughan[1]*, *Paulina Cetina-Heredia*[1], *Nina Ribbat*[1] and *Iain M. Suthers*[2]

[1] Coastal and Regional Oceanography Lab, School of Mathematics and Statistics, University of New South Wales, Sydney, NSW, Australia, [2] School of Biological Earth and Environmental Sciences, University of New South Wales, Sydney, NSW, Australia

The region where the East Australian Current (EAC) separates from the coast is dynamic and the shelf circulation is impacted by the interplay of the western boundary current and its eddy field with the coastal ocean. This interaction can drive upwelling, retention or export. Hence understanding the connection between offshore waters and the inner shelf is needed as it influences the productivity potential of valuable coastal rocky reefs. Near urban centres, artificial reefs enhance fishing opportunities in coastal waters, however these reefs are located without consideration of the productivity potential of adjacent waters. Here we identify three dominant modes of mesoscale circulation in the EAC separation region ($\sim$ 31.5 – 34.5°S); the 'EAC mode' which dominates the flow in the poleward direction, and two eddy modes, the 'EAC eddy mode' and the 'Eddy dipole mode', which are determined by the configuration of a cyclonic and anticyclonic eddy and the relationship with the separated EAC jet. We use a Lagrangian approach to reveal the transport pathways across the shelf to understand the impact of the mesoscale circulation modes and to explore the productivity potential of the coastal waters. We investigate the origin (position and depth) of the water that arrives at the inner-mid shelf over a 21-day period (the plankton productivity timescale). We show that the proportion of water that is upwelled from below the euphotic zone varies spatially, and with each mesoscale circulation mode. Additionally, shelf transport timescales and pathways are also impacted by the mesoscale circulation. The highest proportion of upwelling (70%) occurs upstream of 32.5°S, associated with the EAC jet separation, with vertical displacements of 70–120 m. From 33 to 33.5°S, water comes from offshore above the euphotic layer, and shelf transport timescales are longest. The region of highest retention over the inner shelf is immediately downstream of the EAC separation region. The position of the EAC jet and the location of the cyclonic eddy determines the variability in shelf-ocean interactions and the productivity of shelf waters. These results are useful for understanding productivity of temperate rocky reefs in general and specifically for fisheries enhancements along an increasingly urbanised coast.

Keywords: East Australian Current System, water transport pathways, Hawkesbury Shelf, Lagrangian particle tracking, Great Southern Reef, coastal productivity, cross-shelf exchange, eddies

OPEN ACCESS

Edited by:
William Savidge, University of Georgia, United States

Reviewed by:
Pierrick Penven, Institut de Recherche pour le Développement (IRD), France
Andrea Cucco, National Research Council (CNR), Italy

***Correspondence:**
Moninya Roughan
mroughan@unsw.edu.au

Specialty section:
This article was submitted to Coastal Ocean Processes, a section of the journal Frontiers in Marine Science

Received: *05 October 2021*
Accepted: *06 December 2021*
Published: *07 January 2022*

Citation:
Roughan M, Cetina-Heredia P, Ribbat N and Suthers IM (2022) Shelf Transport Pathways Adjacent to the East Australian Current Reveal Sources of Productivity for Coastal Reefs. Front. Mar. Sci. 8:789687. doi: 10.3389/fmars.2021.789687

1. INTRODUCTION

Production on the continental shelf—and the proximity to ports and markets—is why more than 90% of the global fisheries catch is harvested from continental shelves (Pauly et al., 2002). Further inshore, the valuable coastal rocky reefs support a productive habitat which relies on the delivery of plankton to the reef (Holland et al., 2020). In particular, the delivery of zooplankton, is essential for fisheries production as zooplankton link primary production with higher trophic levels and fisheries (Marshak and Link, 2021).

Phytoplankton and zooplankton growth responds when deep nutrient rich water is uplifted (Brink, 2016) over timescales of 7–21 days (Mongin et al., 2011; Rocha et al., 2019). Zooplankton production advected from upstream of a coastal reef provides a food source for vast schools of small forage fish (Truong et al., 2017; Morais and Bellwood, 2019). The coastal reefs of southeastern Australia have great socio-economic value, but are experiencing environmental stress due to urbanisation and climate change (Bennett et al., 2015). Additionally, demands of growing coastal populations for fresh seafood have impacted the productivity of many coastal ecosystems Chou (1997). Therefore, understanding the physical oceanographic setting, including the source of water reaching the inner shelf and coastal reefs, the shelf transport pathways, residence times and their temporal variability is necessary for understanding the productivity and sustainability of temperate rocky reefs.

To enhance natural reef habitats and local fish stocks, artificial reefs are increasingly being deployed to promote ocean productivity, and increase recreational fishing opportunities for the adjacent urban populations (Champion et al., 2015; Keller et al., 2017). In 2011, Australia's first purpose designed coastal artificial reef was deployed off the coast of Sydney, Australia (33.9°S 151.3°E, **Figure 1**). By 2020, nine new clusters of designed reefs had been deployed along southeastern Australia. However, little consideration has been given to the oceanographic setting and the pathway of water to the reefs when choosing deployment locations.

The circulation along southeastern Australia is generally poleward (Godfrey et al., 1980) influenced by the East Australian Current (EAC) and its eddy field (**Figure 1**) downstream of its separation from the coast (31 − 32.5°S). It is thought that the narrowing of the shelf at Smoky Cape (31°S) and acceleration of the jet prior to separation drives upwelling (Oke and Middleton, 2001; Roughan and Middleton, 2002) that may contribute to productivity over the Hawkesbury Shelf. South of the EAC separation the Hawkesbury Shelf broadens, and the inner shelf circulation (from the coast to the 50 m isobath) is fairly coherent in the along shore (Ribbat et al., 2020b). Nevertheless, the influence of EAC jet drives a dominant along-shore (poleward) transport and the eddy field drives an intermittent cross-shelf transport and even northward flow facilitated by eddy dipoles (Archer et al., 2020; Malan et al., 2020; Ribbat et al., 2020b). Eddying in the region has been shown to be increasing (Li et al., 2021a,b). Thus, the origin of waters flowing across the shelf (e.g., inshore vs. offshore, shallow vs. deep) may be dictated by the mesoscale circulation.

The EAC and its eddies have been shown to influence plankton abundance and cross-shelf phytoplankton composition and distribution, (Armbrecht et al., 2014, 2015). Both modelling (Roughan et al., 2011; Cetina-Heredia et al., 2019a,b) and observational studies (Everett et al., 2015; Roughan et al., 2017)

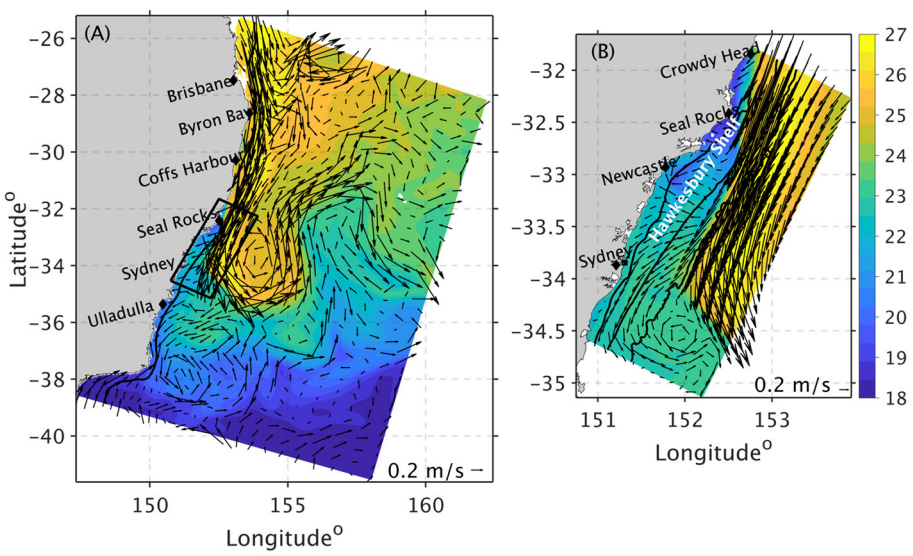

FIGURE 1 | Maps of sea surface temperature (°C) and surface velocity vectors along the east coast of Australia for 9th Jan 2013 shown in **(A)** the EAC-ROMS parent model domain described by Kerry et al. (2016), where the black rectangle shows the domain of the HSM model and the black solid line indicates the 2,000 m isobaths. **(B)** the HSM model domain described by Ribbat et al. (2020a,b) and the location of the Hawkesbury Shelf, black solid lines indicate the 100, 200, and 2,000 m isobaths. The black dot by the coast of Sydney indicates the position of the first coastal artificial reef (OAR).

have revealed the influence of the EAC and its eddies in the supply and/or export of plankton and larvae to or from the shelf. Hence understanding the shelf circulation and its variability is important for understanding delivery of nutrients and plankton to inner shelf waters and the distribution of zooplankton.

Lagrangian particle tracking driven by velocity outputs from a hydrodynamic ocean circulation model is a useful tool with which to investigate the transport pathways of water and particulates in space and time (e.g., Roughan et al., 2003, 2011; Cowen et al., 2006; Cetina-Heredia et al., 2019). Passive particles can be used to represent zooplankton (Roughan et al., 2005a; Cetina-Heredia et al., 2019b; Norrie et al., 2020), nutrients (e.g., Cetina-Heredia et al., 2018), kelp (e.g Coleman et al., 2011, 2013), watermasses (Roughan et al., 2003; Cetina-Heredia et al., 2014), oil (Paris et al., 2012) or other tracers in order to identify typical dispersal pathways (van Sebille et al., 2018) under present and future scenarios (e.g., Cetina-Heredia et al., 2015).

In this study we identify the dominant modes of circulation over the Hawkesbury Shelf offshore of the large Australian cities of Newcastle and Sydney and the Hawkesbury River (**Figure 1B**). We use Lagrangian particle tracking to identify the transport pathways of water flowing across the shelf. We quantify the water sources (position and depth) over a representative 2 year period (2012-2013) and explore the connection to mesoscale circulation of the EAC and its eddy field (section 3) during different circulation scenarios.

By revealing the oceanographic processes that determine the source of water 7–21 days prior to arrival at the inner shelf we aid understanding of the shelf productivity potential. In section 4 these results are placed in the context of coastal productivity, for both natural and artificial reefs. Our technique may be of benefit when selecting locations for placement of additional artificial reefs in the future for maximising biological productivity and efficiency.

2. METHODS

2.1. The Study Site

The study region is located on the continental shelf, between 31.5 and 34.5°S (**Figures 1A,B**) off southeastern Australia. The region is downstream of the typical EAC separation point (Cetina-Heredia et al., 2014; Ribbat et al., 2020b), it encompasses the productive Hawkesbury Bioregion and is offshore of Australia's largest city Sydney. A purpose built coastal artificial reef (named the OAR) is located 1.2 km off the coast of Sydney (33°50'S, 151°17.9'E; **Figure 1B**) in a water depth of 38 m. It is a 40 tonne steel structure that extends to within approximately 26 m of the surface (Champion et al., 2015), designed to increase fishing opportunities.

2.2. The Hawkesbury Shelf Hydrodynamic Model (HSM)

We use velocity outputs from a high-resolution configuration of the Regional Ocean Modelling System (ROMS, V3.4, www.myroms.org) for the Hawkesbury Shelf region. The model domain extends from 31.5 to 34.5°S off SE Australia (**Figure 1B**) and is referred to as the Hawkesbury Shelf Model (HSM) which is described fully in Ribbat et al. (2020a,b). The HSM has a spatial resolution of 750 m, a total of 197 x 477 grid cells, 30 vertical s-layers and 2 h velocity outputs. The HSM is nested inside a 2.5-6 km data assimilating reanalysis of the EAC System (Kerry et al., 2016, 2020), the parent model (EAC-ROMS, **Figure 1A**), and represents the circulation on the shelf for a 2 year period between January 1, 2012 and December 30, 2013. The use of data assimilation in the parent model ensures a realistic depiction of the mesoscale flow for the time period (Kerry et al., 2016, 2018), which makes it ideal for use as boundary conditions.

The nested HSM includes tidal forcing at the boundaries, which is important in coastal regions such as this. The high spatial resolution is needed to ensure that we can resolve the circulation variability over both the inner and outer shelf and to ensure that the bathymetry over the shelf is realistic. Freshwater inflow is generally negligible in this region (Kerry et al., 2016; Ribbat et al., 2020b) and hence has not been included. The full model configuration and validation is described in Ribbat et al. (2020b) who showed that it represents the circulation and temperatures over the shelf region when validated against moored and satellite observations of velocity and temperature.

2.3. Lagrangian Trajectories to Simulate Transport Pathways

We simulate the Lagrangian transport pathways across the shelf through Lagrangian particle trajectory modelling. Particles are seeded throughout the model domain, and are advected offline using the Connectivity Modelling System (CMS) (Paris et al., 2013). CMS uses a fourth order Runge-Kutta advection scheme based on the 3D velocity outputs obtained from the hydrodynamic model. CMS has been used successfully for a wide range of applications in the EAC region including to diagnose watermass transport (Cetina-Heredia et al., 2014, 2019), transport of lobster larvae (Cetina-Heredia et al., 2015, 2019b), and to investigate marine park connectivity (Coleman et al., 2017).

Velocity outputs from the HSM were converted from the ROMS s-grid to a regular z-level grid for compatibility with CMS using 62 vertical layers. A variable vertical resolution was used for the conversion to z-levels, with 2 m resolution in the upper 40 m, 10 m between 40 and 400 m and 100 m from 400 m to the bottom. This conversion is reasonable as the vertical de-correlation length scale has been shown to be 8 m in the region (Roughan et al., 2013, 2015) and our analysis is focused on shelf scales to depths of 200 m. In order to parameterize flow at scales finer than the HSM model (750 m) we use a horizontal diffusivity coefficient of 0.416 m^2 s^{-1} following Okubo (1971). Diffusion coefficients derived from Okubo (1971) have previously been used within CMS to parameterize the impact of flow at spatial scales smaller than modelled outputs along southeast Australia (Cetina-Heredia et al., 2014, 2015, 2019,b).

In order to explore the pathway and origin of the waters that flow across the shelf, particles were advected backwards in time from their release site and tracked for up to 21 days. By releasing particles along the coast over the shelf and tracking them backward in time, we are able to identify the origin (position

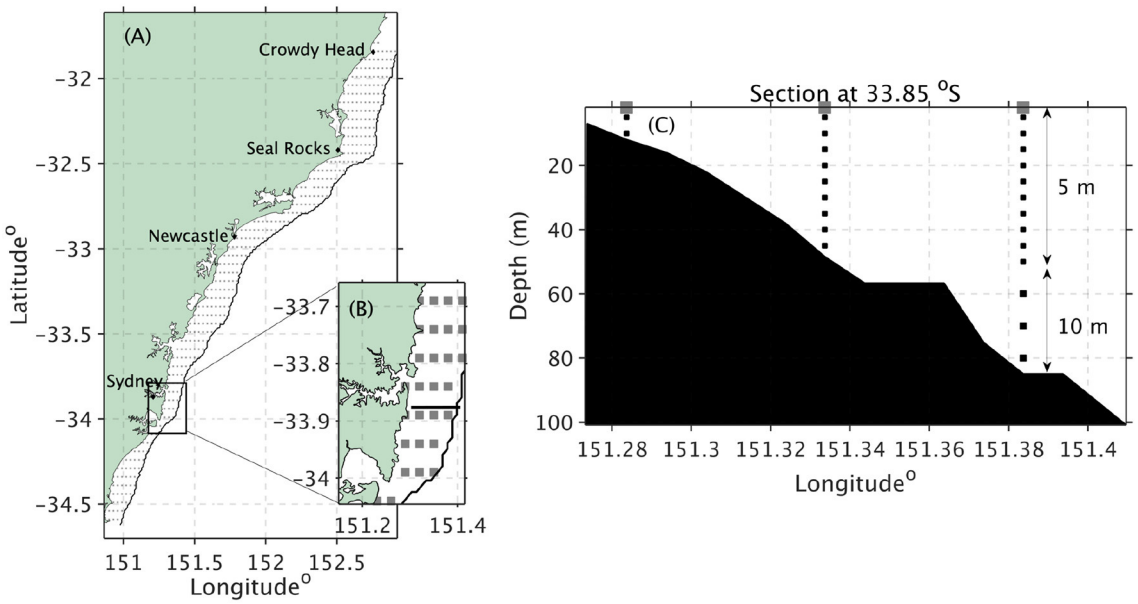

FIGURE 2 | Schematic diagram showing map of particle release locations. **(A)** Surface map of particle release sites along the HSM model domain. The grey squares show the release sites from the coast to the 100 m isobath. **(B)** Zoom in on the Sydney region to show the particle release positions and the location of the transect shown in **(C)**. **(C)** The depth structure of the releases across the inner shelf (black dots), particles are seeded every 5 m from the surface to 50 m, and 10 m from 50 to 100 m.

and depth) of water reaching the inner-mid shelf (0–100 m) and the water transport pathways across the shelf. Using these data we explore a) shelf regions that receive water from below the euphotic zone, b) shelf regions that receive upwelled water and the depth from which it was upwelled, and c) the amount of time that water spent travelling across the shelf where it can be depleted of plankton by feeding of fish and invertebrates. We also explore the impact of different circulation scenarios.

Particles were released throughout the model domain (31.5°S to 34.5°S), from the coastline to the 100 m isobath. The particles are released every 5th along-shore grid cell (3.75 km) and every 3rd across-shelf (2.25 km) grid cell, with a depth interval of every 5 m through the water column from the surface to 50 m and then every 10 m (50 m and deeper) as shown in **Figures 2A,B**. Particles were released at 2-h intervals over the 2 year period and tracked backwards for 21 days. To understand the pathway the particles took across the shelf and to quantify the uplift, the positions of all particles (i.e., latitude, longitude and depth) were recorded every 6 h for 21 days. We use particle tracking results from the full 2 year period, as well as results from three circulation case studies to explore the particle trajectories over the shelf. In each of the case studies we use the particle trajectories over a 21 day period, centred on the specific dates in **Figures 3G–I** (explained further in section 3.1).

3. RESULTS

3.1. Oceanographic Context

The results of the hydrodynamic model simulations show the currents and temperatures over the Hawkesbury Shelf (**Figure 3**). We compare the dominant modes of circulation variability in the HSM domain with satellite derived observations of geostrophic velocity from AVISO (over $\sim$ 25 years from 1994 – 2019). Three dominant circulation modes (calculated as empirical orthogonal functions) are shown in **Figures 3A–F**. We identify the first mode as the 'EAC mode' where the system is dominated by the poleward flowing EAC, representing 47.3% of the variance over the AVISO record and 53.8% of the variance over the 2012 – 2013 HSM period. The second is the 'EAC eddy mode' where the EAC separates in the north of our domain, and a cyclonic eddy is over the shelf (representing 20.1 and 12.4% of the variance in AVISO and HSM, respectively). The third mode is the 'Eddy dipole mode' where an anticyclone/cyclone eddy dipole lies downstream of the EAC separation (representing 13.4 and 10.5% of the variance, respectively). It is expected that there is some difference in the percentage variability explained by the long term AVISO observations and the 2 year HSM run. However, the first three modes identified in our 2 year period are representative of the typical circulation modes as shown. Hence we have confidence using the outputs of this model configuration to investigate cross shelf transport.

3.2. Circulation Case Studies

We use the circulation modes identified above to guide 3 case studies where we explore the impact of mesoscale circulation on the shelf water origin, depth and shelf transport pathways and timescales. A snapshot of the circulation representing each of the case studies is shown in **Figures 3G–I**. For the particle tracking case studies we use the particle trajectories over a 21 day period, centred on the snapshots shown.

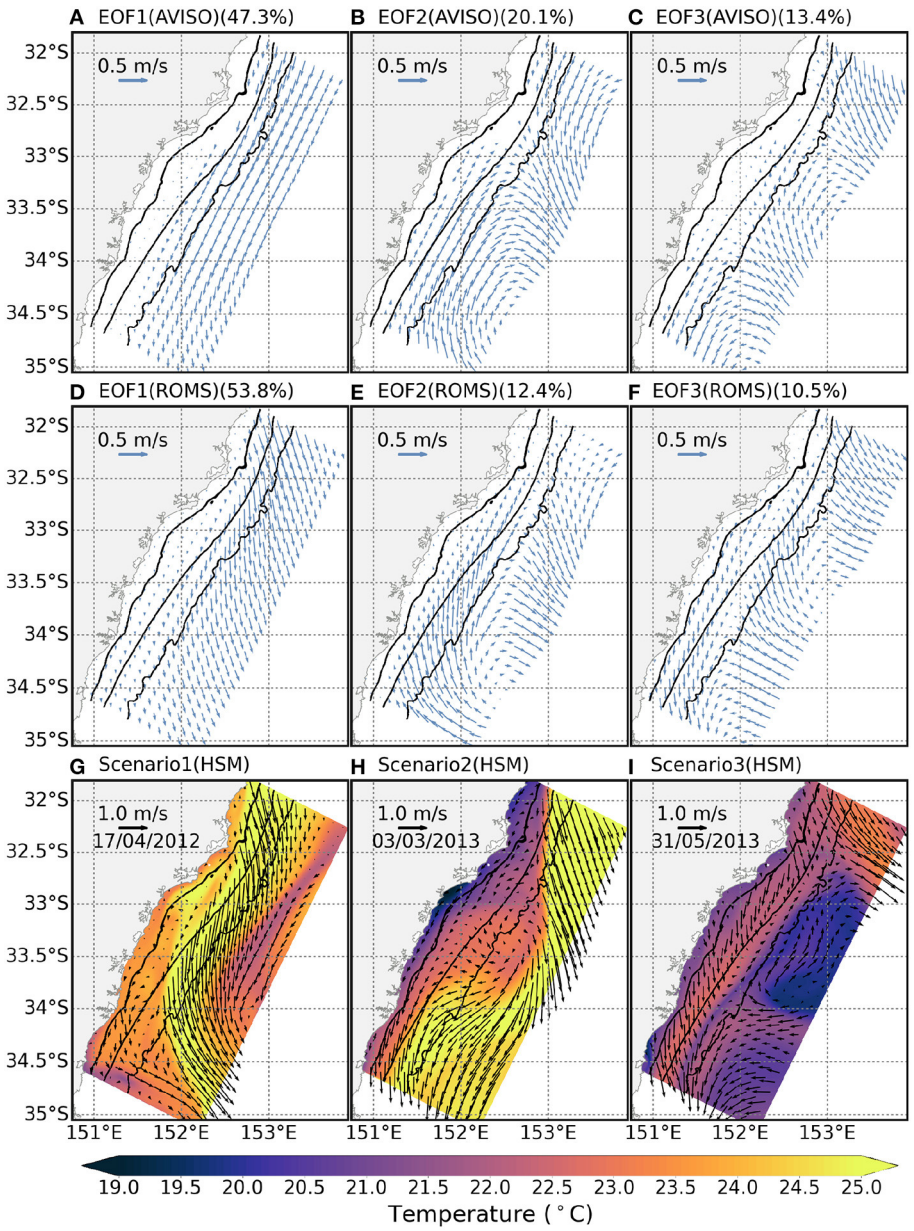

FIGURE 3 | (A–C) Empirical Orthogonal Functions (EOFs) of geostrophic velocity from AVISO, **(D–F)** EOFs from surface velocity from the HSM, percentage of variance explained by each mode is shown in the title. **(G–I)** Snapshots of surface currents and sea surface temperature for three dates as shown in the panels. Solid black lines show the 100, 200, and 2,000 m isobaths.

Figures 3G–I shows that velocities can reach a maximum of 1.5 m s^{-1} in the north of the domain in all three modes driven by the EAC jet. Flows are weaker in the southern half of the domain, and northward flow occurs associated with the position of a cyclonic eddy as seen in circulation mode 2 and mode 3 (**Figures 3D–F**). It is the position of the cyclonic eddy and its positioning with respect to the jet and the anticyclone that determine mode 2 (jet and cyclone) and mode three (jet, cyclone anticyclone) and therefore the direction of the coastal currents.

Snapshots of sea surface temperature (SST) during each of the case studies representing each of the three circulation modes are shown in **Figures 3G–I**. SST is warmest in the northern part of the model domain, under the influence of the poleward flowing EAC and along the inner shelf temperatures are lower. SST is a minimum when shelf waters are influenced by the cyclonic eddies in mode 2 and mode 3. The Eddy dipole case study is centred on a cyclonic eddy during late Autumn showing minimum temperatures of 19 — 20°C (**Figure 3I**).

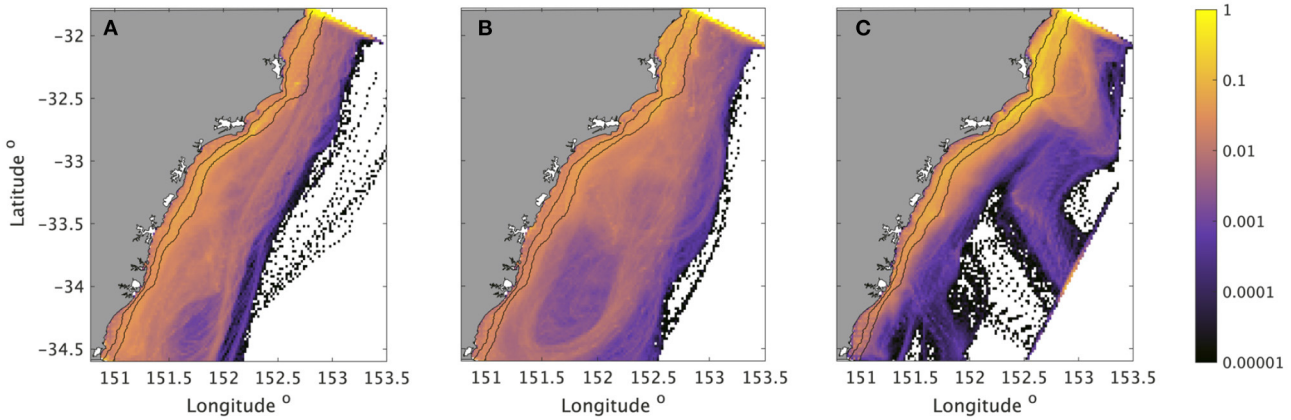

FIGURE 4 | Example shelf transport pathways from particles released by the coast and backtracked in time for up to 21 days illustrated through probability density maps (logarithmic scale as a percentage of particles released). Trajectories are shown for each of the three case studies representing the 3 circulation modes **(A)** EAC mode, **(B)** EAC eddy mode and **(C)** Eddy dipole mode. The black solid lines indicate the 50 and 100 m isobath, respectively.

3.3. Shelf Transport Pathways

Probability density maps were constructed using the backward trajectories from the Lagrangian simulations. These maps represent the probability that a particle will pass through a location over the given time period, and it is expressed as a percentage of the total number of particles released (Mitarai et al., 2009; Roughan et al., 2011). It follows that a high value indicates a greater percentage of particles crossing the grid cell over the specified time frame (Mitarai et al., 2009) and shows the likelihood that water has come from this region (Roughan et al., 2011). The variability in the shelf transport pathways is demonstrated in the probability density maps in **Figure 4** for each of our three case studies that represent the circulation modes: EAC (mode 1), EAC eddy (mode 2) and Eddy dipole (mode 3) as shown in **Figures 3G–I**.

3.4. Across-Shelf Distribution and Source of Inner Shelf Waters

Knowing the source of inner shelf waters gives an indication of productivity potential. The horizontal position (latitude, longitude, depth) of each particle is recorded along their backward trajectory across the shelf and is classified as inshore (coast-50 m), mid-shelf (50–100 m) or offshore (100 m or deeper) based on the water depth along the trajectory. Using all the release data, the percentage of particles found in each of the shelf regions is then determined at 7, 14, and 21 days prior to reaching the coast to give an indication of which section of the shelf particles were sourced. We show the position at origin (by percentage) of particles that arrive between the coast and the 100 m isobath in **Figure 5** using release data for the entire 2 years.

Results reveal that the vast majority of particles that arrive at the coast (60 − 80%) were sourced from the inner shelf over the 3 timescales (7, 14, and 21 days, shown in **Figures 5A–C**, respectively as yellow) from 31.8 − 33.8°S. For waters arriving offshore of the 50 m isobath (**Figure 5D**) ∼ 50% were sourced from the mid-shelf in the 7 day time frame, with offshore sources (60 − 70%) for waters that arrive between 33 and 33.5°S over 14–21 days (**Figures 5H,I**).

3.5. Time Spent Across the Shelf

We explore the time that particles spent over different parts of the shelf (inner shelf, mid-shelf, offshore) which helps us understand the productivity potential as predation is more likely to occur in shallow waters, i.e., over inner shelf rocky reef environments than in offshore waters or at depth and over longer timescales. We assess the impact of the different mesoscale circulation modes on the time particles spent in the 3 across-shelf regions in each of our 3 circulation scenarios (**Figures 3G–I**). The number of days a particle spent within each across-shelf region (inshore, mid-shelf and offshore) over the preceding 21 days was counted and is shown in **Figure 6** for each of the circulation case studies that represent the EAC (mode 1), EAC Eddy (mode 2) and Eddy dipole (mode 3).

For the EAC and EAC eddy modes, water reaching the shelf north of 33 and 32°S, respectively, spent most time mid-shelf; polewards of these latitudes, water spent most of the time offshore before being brought onshore. In contrast, for the Eddy dipole mode, water spent most time in the mid-shelf throughout the domain indicating the influence of the dipole on retention. For all 3 modes, the water spent a short time over the inner shelf (3 − 6 days), with the longest timescales in the dipole mode.

Using all particles released over the 21 days of each case study, we calculated the time taken for the particles to reach the boundary along its backwards trajectory. This gives an estimate of time spent in the domain. For the three circulation mode case studies we get mean residence times of 10 ± 7.5, 12 ± 8.8 and 13±7.5 days, with 69, 63, and 76% of particles leaving the domain, respectively. This means that in the Eddy dipole mode (3), water is retained for up to 3 days longer on the shelf, and that in the EAC eddy mode (2) the most number of particles are retained.

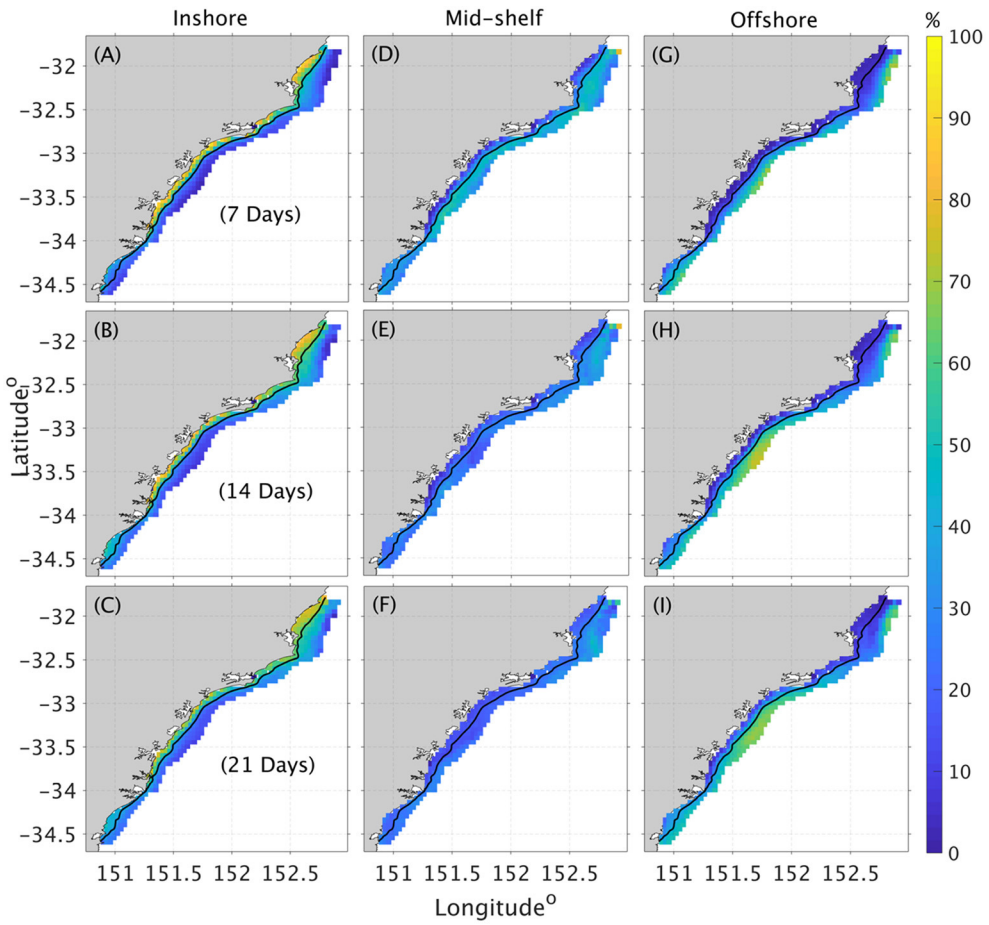

FIGURE 5 | Percentage of simulated particles arriving at each grid cell along the coastal (for particles released between the coast and the 100 m isobath) that come from: **(A–C)**, inner shelf region (0–50 m); **(D–F)** mid-shelf region (50–100 m) and **(G–I)** offshore region (>100 m) from 7, 14, and 21 days prior (top to bottom). The black solid line shows the 50 m isobath.

3.6. Vertical Distribution of Source Waters That Reach the Inner Shelf

Investigating the depth of the source waters that reach the inner shelf region allows us to further understand the potential productivity of the water flowing across the shelf and to identify regions more likely to receive upwelled water (with potential for higher nutrient concentration). Using trajectories of all releases adjacent to the coastline, depths recorded 21 days prior to the release date were used to identify the depth range (in intervals of 10 m) where waters that arrived at the inner shelf originated (**Figure 7**).

The histograms for all particle trajectories over the 2 year period show the proportion of upwelled waters (**Figure 7**). Overwhelmingly, the majority of the water that arrives at the coast originates at depths of 0–20 m over 7, 14, and 21 days. Some upwelled waters arrive at the coast from depths greater than 60 m in the northern and southern extents of the model domain, more so on the 7 day timescale. In the middle of the domain, from 32 to 34°S upwelling is less prevalent.

3.7. Impact of Mesoscale Circulation on Vertical Distribution of Source Waters

For each of our 3 circulation case studies we quantify the proportion of water that comes from depths below the euphotic layer 21 days prior (**Figures 8A–C**), considered to be ∼ 50 m in this region (Rocha et al., 2019). Using trajectories of releases adjacent to the seafloor, we compare the coastal release depth (final position) and the depth 21 days before (source depth), to discern if water was upwelled or downwelled (**Figures 8D–F**). We then explore the vertical displacement averaged across all particles that were upwelled (**Figures 8G–I**).

During the EAC scenario (mode 1), when the poleward alongshore flow is strong, waters are sourced from below the euphotic depth (**Figures 8A,D,G**), upwelling is persistent the length of the study area and across the mid and outer shelf. Vertical displacements are a maximum (80 – 120 m) in the southern part of the domain (from 33.5 to 34.5°S).

During the EAC eddy scenario (mode 2, **Figures 8B,E,H**) only 20–30% of the waters are from below the euphotic depth,

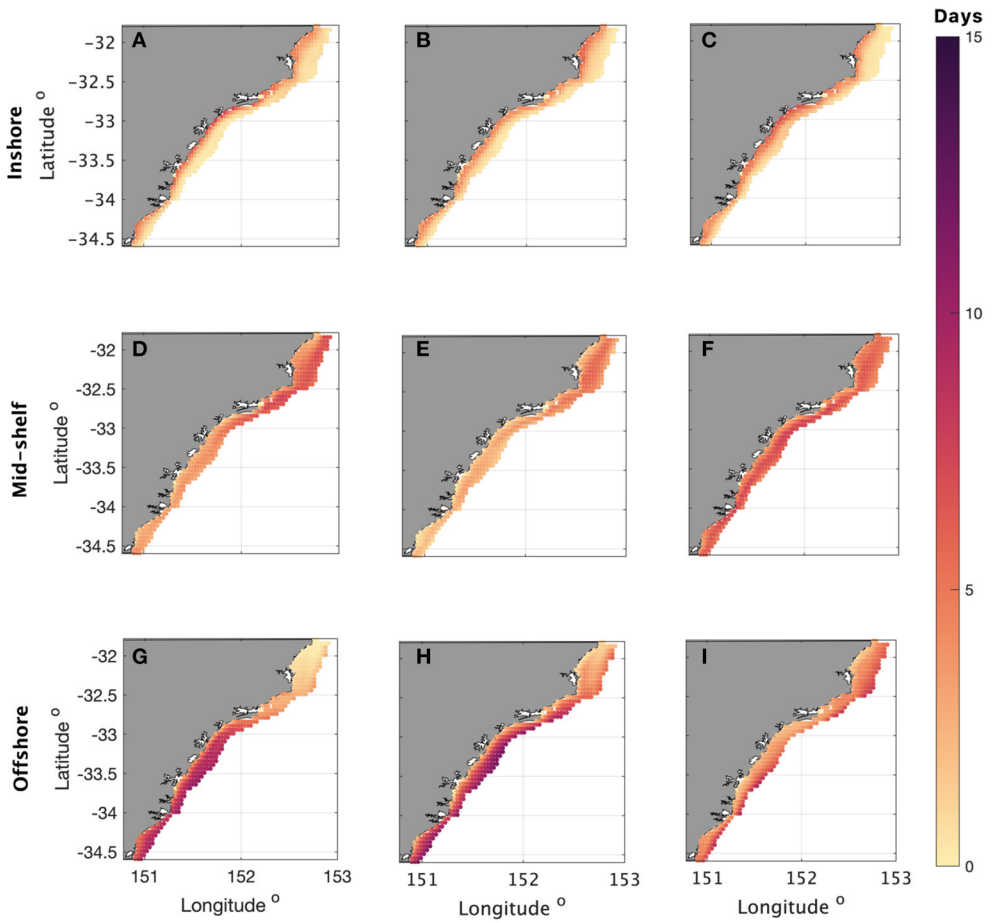

FIGURE 6 | Quantification of the number of days the water spent in each region across the shelf before arriving at the coast. i.e., the time spent inshore—between the coast and the 50 m isobath **(A–C)**, over the mid-shelf, between the 50 and 100 m isobaths **(D–F)**, and offshore, between the 100 m isobath and deeper **(G–I)**, shown for each of the three case studies representing the 3 circulation modes ('EAC mode', 'EAC eddy mode', and 'Eddy dipole mode', respectively left to right). The number of days shown for each grid cell was computed as an average across all the particles released at each coastal grid cell.

although across the mid-outer shelf, much of the bottom waters are sourced from below, with vertical displacements of 40–60 m. In the EAC dipole scenario, waters come from below the euphotic depth least often, but waters that are upwelled involve displacements of over 80 m and maximum displacements occur in the northern region of our study area, between 32° and 32.5°S (**Figures 8C,F,J**).

3.8. Distance Travelled

We explore the linear distance (L) travelled by the water parcels i.e., the distance between the release location and the particle's position 7, 14, and 21 days before. Similarly, we measured the distance along the backward water trajectory (T) of each water parcel (particle). The distances were grouped in 30 km bins to show how far a watermass has travelled in the preceding days. Additionally, the ratio between the linear and along-trajectory distance (L/T) was computed to compare how direct the trajectories were; a value of one implies the trajectory was straight, whereas a lower value shows the parcel trajectory was more convoluted or eddying (**Figure 9**). For this analysis we use particles released at the location of Sydney's coastal artificial reef (OAR) as shown in **Figure 7** in the southern end of our domain.

Over 7 days prior to reaching the OAR, the linear distance to the source ranges 30–60 km, and over 21 days the distance ranges 90–120 km (**Figure 9A**). By following the watermass along its trajectory, we observe that the distances actually travelled are more than 50% higher with the majority of particles covering a distance between 180 and 240 km over the 21 days prior to reaching the OAR, with the longest particle paths exceeding 450 km (**Figure 9B**). Interestingly a small percentage of particles that arrived at the inner shelf OAR site travelled up to 600 km. Over the 21 days only 11% of the particles have a linear to along-trajectory distance (L/T) ratio between 0.75 and 1, (vs. 40% over 7 days, **Figure 9C**). This ratio indicates that the longer a parcel is tracked, the more convoluted the path travelled to arrive at the coast, and can indicate increased retention over the shelf.

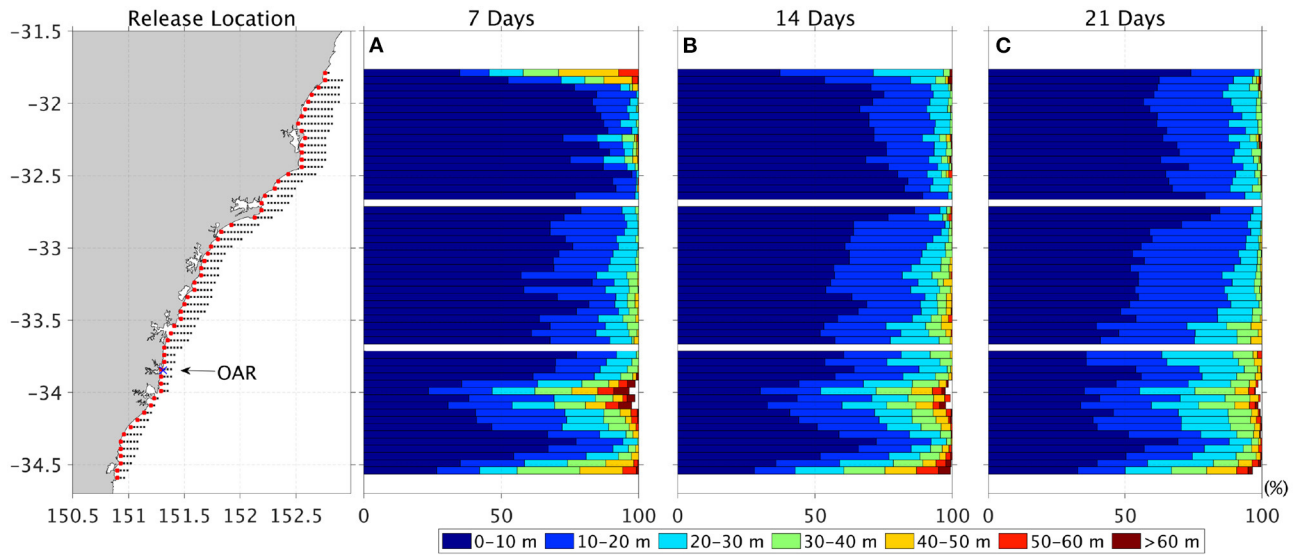

FIGURE 7 | Histograms (by latitude) showing the depth that the waters came from as a percentage of the total. The colors indicate the depth ranges from which the water particles came **(A)** 7, **(B)** 14, and **(C)** 21 days prior to the release date, arriving at the red dots at the coast.

4. DISCUSSION

The origin and transport pathways of water flowing across the inner-mid shelf of the Hawkesbury Bioregion off SE Australia was examined from Lagrangian backtracking simulations to reveal the connection between mesoscale circulation and shelf transport. These trajectories showed dispersal patterns and sources of water parcels reaching the inner-mid shelf, which differed under three different mesoscale circulation patterns. We explore the shelf transport pathways the depth of origin and relationship to upwelling in order to understand the likely productivity of waters flowing across the inner-mid shelf. Here we place the results in the context of water arriving at coastal rocky reefs and Sydney's first coastal artificial reef and discuss possibilities for future positioning of purpose built coastal reefs.

4.1. Impact of Mesoscale Circulation on Shelf Transport Pathways

The EAC varies on 90 – 110 day timescales, associated with mesoscale eddy shedding and a retraction in the EAC separation latitude (Cetina-Heredia et al., 2014). In this region, the mesoscale circulation is characterised by 3 modes, the 'EAC mode', 'EAC eddy mode', and 'Eddy dipole mode', as exemplified in **Figure 3**. These modes were depicted in the schematic diagram of Ribbat et al. (2020b) based on just 2 years of data. However, the similarity between the 3 modes calculated from long term AVISO observations and those from our HSM model **Figure 3**) give confidence in the robustness of the modes, and the use of the model snapshots to explore each of the three scenarios.

These mesoscale dynamics dominate the circulation over the mid-outer shelf, and in the north of the domain which is mostly upstream of the EAC separation. This is consistent with the results of Wood et al. (2016) who showed that the EAC and its eddies drive the outer shelf circulation (**Figure 3**). Our results show that this has an impact on the cross shelf trajectories and water transport pathways (**Figure 4**). When the circulation is Mode 1 (EAC mode), the EAC is strong poleward along the outer shelf, flow is from the north, and eddy impacts are a minimum. Across the inner shelf the water is sourced from the inshore and upstream (**Figures 3**, **4**) particularly on short time scales.

When the EAC separates in the north of the domain (Eddy mode or Eddy dipole mode) water transport pathways are more variable across the shelf and water was sourced from offshore as well as along shore (**Figure 4**). Consistent with the sourcing of waters from offshore in this region, Ribbat et al. (2020b) showed that onshore transport was maximum at about 34°S, during this period. Vertical displacement is also a maximum during EAC transport (mode 1) (**Figure 8C**). These results show that the position of the EAC jet and the location of the cyclonic eddy determines the variability in shelf-ocean interactions in each of these scenarios which has potential to drive the productivity of shelf waters.

4.2. Upwelling and Shelf Transit Timescales

The region that extends from 32 – 32.5°S is a known region of upwelling, driven by the acceleration of the EAC jet and its separation from the coast (Roughan and Middleton, 2002, 2004). An example of this is observed in the snapshot of sea surface temperature and velocity as shown in **Figure 1** and our mode 1 case study (**Figures 3D,G**). From 32 – 32.5°S is the only region in our model domain that consistently receives water from below the euphotic depth over the 2 year period. Ribbat et al. (2020b) showed that during this period, the EAC separated from the coast between 32.5 and 33.5°S up to 70% of the time. This means that

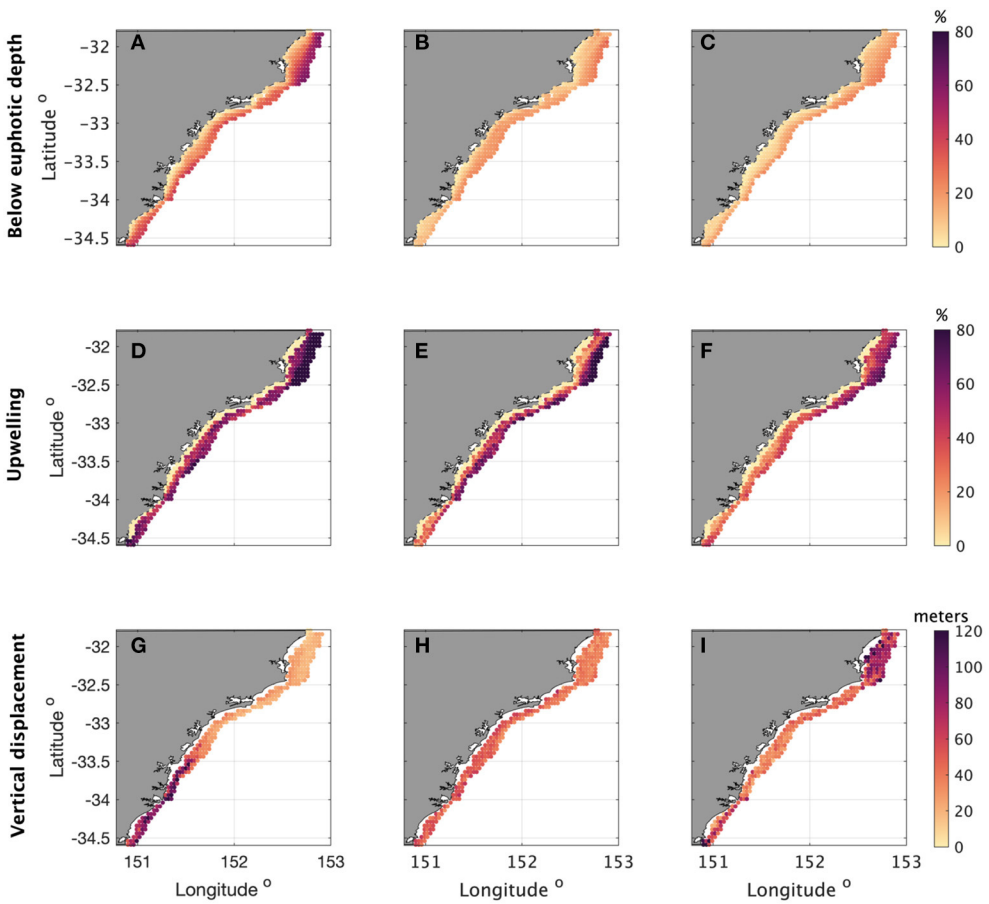

FIGURE 8 | Proportion of water that comes from (below the euphotic depth) **(A–C)**; the proportion of water that was upwelled **(D–F)**; and the mean vertical displacement (meters) of water parcels that were upwelled **(G–I)** for the three case studies, 'EAC mode' (left), 'EAC eddy mode' (middle), and 'Eddy dipole mode' (right) columns. The proportion of water below the euphotic depth was computed across particles released throughout the water column. The proportion of water that was upwelled was computed only considering the trajectories of particles that were released close to the sea floor.

for much of the simulation, the shelf region from 32 to 32.5°S was considered inshore and upstream of separation. Upwelling in this region is consistent with the results of Schaeffer et al. (2014) who showed that onshore transport in the bottom boundary layer was more intense and frequent upstream of separation than downstream.

From 33 – 33.5°S we show that water comes from offshore (e.g., **Figures 5G–I**), but from above the euphotic layer (**Figures 8A,D,G**) with vertical displacements ranging 10 – 30 m. In this region onshore transport is associated with EAC eddy dipoles (Malan et al., 2020, 2021), which occur regularly in the region. Our results suggest that while onshore transport occurs, waters are not upwelled from depths greater than 50 m. Interestingly however in this region, retention and shelf transit times are longer (**Figures 6B,E,H**) with the mid-shelf having the longest transport pathways of the entire domain. This could help increase the productivity of the region by retaining plankton over the shelf. The transport pathway ratios L/T show the convoluted path that a water parcel could to reach the inner shelf, indicative of increased residence time over the shelf (**Figure 9**). This is important, as in an advection dominated regime some degree of shelf retention is needed for phytoplankton blooms to occur (Roughan et al., 2005b).

The Stockton Bight region immediately downstream of the EAC separation (32.25 – 33.25°S) has been shown to be more productive than other sections of the shelf, at times containing more than 20% of the total shelf chlorophyll (Everett et al., 2014). However, the relationship between EAC circulation modes, water mass variability and chlorophyll concentrations on the shelf is not yet clear. Repeat glider missions collecting hydrographic data through the domain (supported by Australia's Integrated Marine Observing System Roughan et al., 2015; Schaeffer et al., 2016a,b) provide the ideal dataset with which to explore drivers of chlorophyll variability in the EAC separation zone in the future.

4.3. Productivity of Coastal Reefs

The transport and upwelling processes described in our study are a key contributor to the persistent coastal fringe of phytoplankton, referred to on other coasts as the 'green ribbon' (Lucas et al., 2011). This is especially evident inshore of the EAC

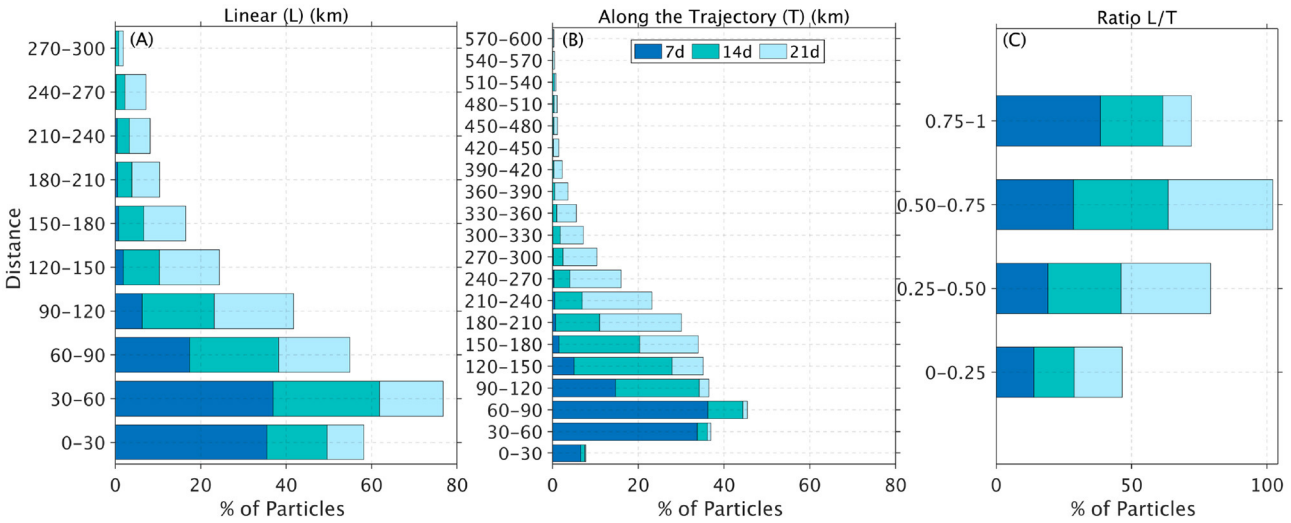

FIGURE 9 | Distance travelled by particles that arrive at the coastal artificial reef (OAR), where particles were back-tracked over 7, 14, and 21 days, presented as a percentage (stacked histogram), showing **(A)** the linear distance (L) from the start to the end point at each time period, **(B)** the total along-trajectory distance (T) travelled by the particle, and **(C)** the ratio between Linear and Trajectory distance L/T for each time period, where a ratio of 1 shows the particle travelled in a straight line. The location of the OAR is shown in **Figure 7**.

separation zone at the northern sector of our domain, which sustains the economically important Hawkesbury Bioregion. This region is exceptionally productive in phytoplankton (Everett et al., 2014) and is the predominant region for eddy formation (Cetina-Heredia et al., 2014; Ribbat et al., 2020b) as well as onshore transport Cetina-Heredia et al. (2019b), Malan et al. (2020). The region therefore benefits from the major EAC / eddy separation processes (Oke and Middleton, 2001; Roughan and Middleton, 2002), delivering nutrients to where the shelf widens to its furthest extent for southeastern Australia. Together, these processes not only underpin the coastal fisheries for this highly urbanised coastline (Holland et al., 2020), but it is known to be a white shark nursery area (Lee et al., 2021). The coastal reefs in this region are part of the Great Southern Reef which refers to Australia's 8000 km coastline of temperate rocky reef, from southern Queensland to Western Australia (Bennett et al., 2015). The associated kelp forest and other macroalgae are highly productive and sustain these valuable ecosystems for a quarter of Australia's population.

The kelp forests and macroalgae are however, only part of the reason for region's productivity. The majority of fish biomass on the valuable temperate reefs in the region is not only based on macroalgae, but on the supply of zooplankton (Truong et al., 2017; Holland et al., 2020). A similarly important process is recognised on tropical coral reefs, referred to as a pelagic subsidy (Morais and Bellwood, 2019). In the case of coastal reefs along southeastern Australia, the phytoplankton which sustains benthic filter feeders (such as sponges, oysters and ascidians) is produced over the previous 7–14 days over the water transport pathway. We determined that the production of zooplankton over the previous 21 days is mostly sourced from 30 to 100 km north. The majority of this production is maintained along the inner shelf, such that schools of small forage fish along the inner shelf may have the potential to reduce zooplankton densities if cross-shelf flows are infrequent.

4.4. Placement of Artificial Reefs

Artificial reefs are often placed within close proximity to the coast to enhance accessibility for both construction logistics, and recreational fishing opportunities (Chou, 1997; Champion et al., 2015). For example, proximity to a population centre with an easy transit to a safe harbour will enhance use by the recreational fishing community. Additionally, local morphological and habitat features may also enhance productivity. Hence, artificial reefs are also often placed in the vicinity of natural reefs (Champion et al., 2015) to aid recruitment and improve connectivity between reefs.

An important factor influencing the productivity of an artificial reef however is the supply of zooplankton for small forage fish, which attract larger fish of interest to the recreational fishing industry (Champion et al., 2015). The likelihood for water to contain zooplankton and nutrients when flowing over an artificial reef can vary depending on its source region and trajectory. Our results show that the Sydney OAR (see **Figure 1B** for location) broadly receives waters from the inner shelf, directly upstream, and that upwelling across this reef is limited, especially when compared to other sites along the shelf. If the reef was located over the mid-shelf region, or further to the south, the productivity potential would likely be increased.

If reefs were to be deployed in upwelling regions, our results suggest reefs should be located in the north of the domain, e.g., from 32 to 32.5°S, although this would not allow sufficient time for zooplankton production. Furthermore, the longer retention times between 33 and 33.5°S mid-shelf are more

suited for retention of zooplankton production, while between 34 and 34.5°S regions close to the coast receive upwelled waters from offshore.

This work is a first step towards understanding Lagrangian transport pathways and timescales across the Hawkesbury Shelf and shows the influence of the mesoscale circulation, which in turn can impact coastal reef productivity. Understanding the spatial and temporal patterns of primary and secondary productivity (phytoplankton and smaller zooplankton) as well as the quantification of the flux of zooplankton in shelf waters will aid future reef placements. Ultimately, a better understanding of zooplankton abundance and delivery to natural and artificial reefs would be beneficial in order to estimate the sustainability of the on-going deployments of artificial reefs.

While socio-economic arguments and proximity to natural reefs and habitat are important when considering the placement of coastal artificial reefs, our results show that knowledge of the predominant shelf transport pathways and upwelling characteristics are also important considerations due to their impact on the productivity potential of the reef. Our findings have implications for the ecosystem basis for other socio-economically valuable temperate reefs adjacent to other western boundary currents, such as off eastern Japan, eastern Florida, and the Natal coast.

DATA AVAILABILITY STATEMENT

The datasets presented in this study can be found in online repositories. The names of the repository/repositories and accession number(s) can be found below: The Hawkesbury Shelf model output used in this study can be found at the Research Data Australia repository at https://doi.org/10.26190/5ec35ca34752e and should be cited as Ribbat et al. (2020a). Satellite data used in **Figure 3** was obtained from https://resources.marine.copernicus.eu/?option=com_csw&view=details&product_id=SEALEVEL_GLO_PHY_L4_REP_OBSERVATIONS_403008_047.

AUTHOR CONTRIBUTIONS

MR and IS conceived the study and developed the conceptual framework, and obtained the funding. NR and PC-H conducted the model runs and generated the figures. PC-H and MR led the analysis. All authors contributed to interpreting the results, writing and editing the manuscript.

FUNDING

NR was partially supported by an Australian Research Council Industry Linkage Project LP120100592 to IS and MR. The EAC-ROMS model development was supported by an Australian Research Council Discovery Project DP140102337 to MR. NR received a tuition fee scholarship from UNSW Sydney.

ACKNOWLEDGMENTS

This research was undertaken with the assistance of resources and services from the National Computational Infrastructure (NCI), which is supported by the Australian Government. This research also includes computations using the computational cluster Katana supported by Research Technology Services at UNSW Sydney. We acknowledge C. Kerry, B. Powell, and S. Rao for assistance with earlier model development, J. Smith for discussions on the OAR and J. Li for AVISO data in **Figure 3**.

REFERENCES

Archer, M., Schaeffer, A., Keating, S., Roughan, M., Holmes, R., and Siegelman, L. (2020). Observations of submesoscale variability and frontal subduction within the mesoscale eddy field of the Tasman Sea. *J. Phys. Oceanogr.* 50, 1509–1529. doi: 10.1175/JPO-D-19-0131.1

Armbrecht, L. H., Roughan, M., Rossi, V., Schaeffer, A., Davies, P. L., Waite, A. M., et al. (2014). Phytoplankton composition under contrasting oceanographic conditions: upwelling and downwelling (Eastern Australia). *Cont. Shelf Res.* 75, 54–67. doi: 10.1016/j.csr.2013.11.024

Armbrecht, L. H., Schaeffeer, A., Roughan, M., and Armand, L. K. (2015). Interactions between seasonality and oceanic forcing drive the phytoplankton variability in the tropical-temperate transition zone (30° S) of Eastern Australia. *J. Mar. Syst.* 144, 92–106. doi: 10.1016/j.jmarsys.2014.11.008

Bennett, S., Wernberg, T., Connell, S. D., Hobday, A. J., Johnson, C. R., and Poloczanska, E. S. (2015). The "Great Southern Reef": social, ecological and economic value of Australia's neglected kelp forests. *Mar. Freshwater Res.* 67, 47–56. doi: 10.1071/MF15232

Brink, K. (2016). Cross-shelf exchange. *Ann. Rev. Mar. Sci.* 8, 59–78. doi: 10.1146/annurev-marine-010814-015717

Cetina-Heredia, P., Roughan, M., Liggins, G., Coleman, M. A., and Jeffs, A. (2019a). Correction: Mesoscale circulation determines broad spatio-temporal settlement patterns of lobster *PLoS ONE.* 14:2 (e02214996). doi: 10.1371/journal.pone.0214996

Cetina-Heredia, P., Roughan, M., Liggins, G., Coleman, M. A., and Jeffs, A. (2019b). Mesoscale circulation determines broad spatio-temporal settlement patterns of lobster. P*LoS ONE.* 14:e0211722. doi: 10.1371/journal.pone.0211722

Cetina-Heredia, P., Roughan, M., Sebille, E., Keating, S., and Brassington, G. B. (2019). Retention and leakage of water by mesoscale eddies in the East Australian Current System. *J. Geophys. Res. Oceans* 124, 2485–2500. doi: 10.1029/2018JC014482

Cetina-Heredia, P., Roughan, M., van Sebille, E., and Coleman, M. A. (2014). Long-term trends in the East Australian Current separation latitude and eddy driven transport. *J. Geophys. Res. Oceans* 119, 4351–4366. doi: 10.1002/2014JC010071

Cetina-Heredia, P., Roughan, M., Van Sebille, E., Feng, M., and Coleman, M. A. (2015). Strengthened currents override the effect of warming on lobster larval dispersal and survival. *Glob. Chang Biol.* 21, 4377–4386. doi: 10.1111/gcb.13063

Cetina-Heredia, P., van Sebille, E., Matear, R. J., and Roughan, M. (2018). Nitrate sources, supply, and phytoplankton growth in the Great Australian Bight: an eulerian-lagrangian modeling approach. *J. Geophys. Res. Oceans* 123, 759–772. doi: 10.1002/2017JC013542

Champion, C., Suthers, I. M., and Smith, J. A. (2015). Zooplanktivory is a key process for fish production on a coastal artificial reef. *Mar. Ecol. Prog. Ser.* 541, 1–14. doi: 10.3354/meps11529

Chou, L. M. (1997). Artificial reefs of Southeast Asia-do they enhance or degrade the marine environment? *Environ. Monit. Assess* 44, 45–52. doi: 10.1023/A:1005759818050

Coleman, M. A., Cetina-Heredia, P., Roughan, M., Feng, M., van Sebille, E., and Kelaher, B. P. (2017). Anticipating changes to future connectivity within a network of marine protected areas. *Glob. Chang Biol.* 23, 3533–3542. doi: 10.1111/gcb.13634

Coleman, M. A., Feng, M., Roughan, M., Cetina-Heredia, P., and Connell, S. D. (2013). Temperate shelf water dispersal by Australian boundary currents: implications for population connectivity. *Limnol. Oceanogr. Fluids Environ.* 3, 295–309. doi: 10.1215/21573689-2409306

Coleman, M. A., Roughan, M., Macdonald, H. S., Connell, S. D., Gillanders, B. M., Kelaher, B. P., et al. (2011). Variation in the strength of continental boundary currents determines continent-wide connectivity in kelp. *J. Ecol.* 99, 1026–1032. doi: 10.1111/j.1365-2745.2011.01822.x

Cowen, R. K., Paris, C. B., and Srinivasan, A. (2006). Scaling of connectivity in marine populations. *Science* 311, 522–527. doi: 10.1126/science.1122039

Everett, J. D., Baird, M. E., Roughan, M., Suthers, I. M., and Doblin, M. A. (2014). Relative impact of seasonal and oceanographic drivers on surface chlorophyll a along a Western Boundary Current. *Prog. Oceanogr.* 120, 340–351. doi: 10.1016/j.pocean.2013.10.016

Everett, J. D., Macdonald, H., Baird, M. E., Humphries, J., Roughan, M., and Suthers, I. M. (2015). Cyclonic entrainment of preconditioned shelf waters into a frontal eddy. *J. Geophys. Res. Oceans* 120, 677–691. doi: 10.1002/2014JC010301

Godfrey, J., Cresswell, G., Golding, T., Pearce, A., and Boyd, R. (1980). The separation of the East Australian Current. *J. Phys. Oceanogr.* 10, 430–440. doi: 10.1175/1520-0485(1980)010andlt;0430:TSOTEAandgt;2.0.CO;2

Holland, M. M., Smith, J. A., Everett, J. D., Vergés, A., and Suthers, I. M. (2020). Latitudinal patterns in trophic structure of temperate reef-associated fishes and predicted consequences of climate change. *Fish Fish.* 21, 1092–1108. doi: 10.1111/faf.12488

Keller, K., Steffe, A. S., Lowry, M. B., Murphy, J. J., Smith, J. A., and Suthers, I. M. (2017). Estimating the recreational harvest of fish from a nearshore designed artificial reef using a pragmatic approach. *Fish Res.* 187, 158–167. doi: 10.1016/j.fishres.2016.11.022

Kerry, C., Powell, B., Roughan, M., and Oke, P. (2016). Development and evaluation of a high-resolution reanalysis of the East Australian Current region using the regional ocean modelling system (ROMS 3.4) and incremental strong-constraint 4-dimensional variational (IS4D-Var) data assimilation. *Geosci. Model Dev.* 9, 3779–3801. doi: 10.5194/gmd-9-3779-2016

Kerry, C., Roughan, M., and Powell, B. (2018). Observation impact in a regional reanalysis of the East Australian Current System. *J. Geophys. Res. Oceans* 123, 7511–7528. doi: 10.1029/2017JC013685

Kerry, C., Roughan, M., Powell, B., and Oke, P. (2020). A high-resolution reanalysis of the East Australian Current System assimilating an unprecedented observational data set using 4D-Var data assimilation over a two-year period (2012-2013). Version 2017. UNSW.dataset, Sydney doi: 10.26190/5ebe1f389dd87

Lee, K. A., Butcher, P. A., Harcourt, R. G., Patterson, T., Peddemors, V. M., Roughan, M., et al. (2021). Oceanographic conditions associated with white shark (*Carcharodon carcharias*) habitat use along eastern Australia. *Mar. Ecol. Prog. Ser.* 659, 143–159. doi: 10.3354/meps13572

Li, J., Roughan, M., and Kerry, C. (2021a). Dynamics of interannual eddy kinetic energy modulations in a Western Boundary Current. *Geophys. Res. Lett.* 48:e2021GL094115. doi: 10.1029/2021GL094115

Li, J., Roughan, M., and Kerry, C. (2021b). Variability and drivers of ocean temperature extremes in a warming western boundary current. *J. Clim.* 1–10. doi: 10.1175/JCLI-D-21-0622.1

Lucas, A. J., Dupont, C. L., Tai, V., Largier, J. L., Palenik, B., and Franks, P. J. S. (2011). The green ribbon: Multiscale physical control of phytoplankton productivity and community structure over a narrow continental shelf. *Limnol. Oceanogr.* 56, 611–626. doi: 10.4319/lo.2011.56.2.0611

Malan, N., Archer, M., Roughan, M., Cetina-Heredia, P., Hemming, M., Rocha, C., et al. (2020). Eddy-driven cross-shelf transport in the East Australian Current separation zone. *J. Geophys. Res. Oceans* 125:e2019JC015613. doi: 10.1029/2019JC015613

Malan, N., Roughan, M., Stanley, G. J., Holmes, R. M., and Li, J. (2021). Quantifying cross-shelf transport in the East Australian Current system: a budget- based approach. *J. Phys. Oceanogr.* [Epub ahead of print].

Marshak, A. R., and Link, J. S. (2021). Primary production ultimately limits fisheries economic performance. *Sci. Rep.* 11, 12154. doi: 10.1038/s41598-021-91599-0

Mitarai, S., Siegel, D. A., Watson, J. R., Dong, C., and McWilliams, J. C. (2009). Quantifying connectivity in the coastal ocean with application to the southern Californian Bight. *J. Geophys. Res.* 114:C10026. doi: 10.1029/2008JC005166

Mongin, M., Matear, R., and Chamberlain, M. (2011). Seasonal and spatial variability of remotely sensed chlorophyll and physical fields in the saz-sense region. *Deep Sea Res. Part II Top. Stud. Oceanogr.* 58, 2082–2093. doi: 10.1016/j.dsr2.2011.06.002

Morais, R. A., and Bellwood, D. R. (2019). Pelagic subsidies underpin fish productivity on a degraded coral reef. *Curr. Biol.* 29, 1521.e6–1527.e6. doi: 10.1016/j.cub.2019.03.044

Norrie, C., Dunphy, B., Roughan, M., Weppe, S., and Lundquist, C. (2020). Spill-over from aquaculture may provide a larval subsidy for the restoration of mussel reefs. *Aquacult. Environ. Interact.* 12, 231–249. doi: 10.3354/aei00363

Oke, P. R., and Middleton, J. H. (2001). Nutrient enrichment off Port Stephens: the role of the East Australian Current. *Cont. Shelf Res.* 21, 587–606. doi: 10.1016/S0278-4343(00)00127-8

Okubo, A. (1971). Oceanic diffusion diagrams. *Deep Sea Res. Oceanogr. Abstracts* 18, 789–802. doi: 10.1016/0011-7471(71)90046-5

Paris, C. B., Helgers, J., van Sebille, E., and Srinivasan, A. (2013). Connectivity modeling system: a probabilistic modeling tool for the multi-scale tracking of biotic and abiotic variability in the ocean. *Environ. Model. Softw.* 42, 47–54. doi: 10.1016/j.envsoft.2012.12.006

Paris, C. B., Hénaff, M. L., Aman, Z. M., Subramaniam, A., Helgers, J., Wang, D.-P., et al. (2012). Evolution of the macondo well blowout: simulating the effects of the circulation and synthetic dispersants on the subsea oil transport. *Environ. Sci. Technol.* 46, 13293–13302. doi: 10.1021/es303197h

Pauly, D., Christensen, V., Guénette, S., Pitcher, T. J., Sumaila, U. R., Walters, C. J., et al. (2002). Towards sustainability in world fisheries. *Nature* 418, 689–695. doi: 10.1038/nature01017

Ribbat, N., Roughan, M., Powell, B., Kerry, C., and Rao, S. (2020a). *A High-Resolution (750m) Free-Running Hydrodynamic Simulation of the Hawkesbury Shelf Region Off Southeastern Australia (2012-2013) using the Regional Ocean Modeling System*. Sydney, SY: UNSW.dataset.

Ribbat, N., Roughan, M., Powell, B., Rao, S., and Kerry, C. (2020b). Transport variability over the Hawkesbury Shelf (31.5–34.5°S) driven by the East Australian Current. *PLoS ONE* 15:e0241622. doi: 10.1371/journal.pone.0241622

Rocha, C., Edwards, C. A., Roughan, M., Cetina-Heredia, P., and Kerry, C. (2019). A high-resolution biogeochemical model (roms 3.4 + bio_fennel) of the East Australian Current system. *Geosci. Model Dev.* 12, 441–456. doi: 10.5194/gmd-12-441-2019

Roughan, M., Keating, S., Schaeffer, A., Cetina-Heredia, P., Rocha, C., Griffin, D., et al. (2017). A tale of two eddies: the bio-physical characteristics of two contrasting cyclonic eddies in the Tasman Sea. *J. Geophys. Res. Oceans.* 2494–2518. doi: 10.1002/2016JC012241

Roughan, M., Macdonald, H. S., Baird, M. E., and Glasby, T. M. (2011). Modelling coastal connectivity in a Western Boundary current: Seasonal and inter-annual variability. *Deep Sea Res. II Top. Stud. Oceanogr.* 58, 628–644. doi: 10.1016/j.dsr2.2010.06.004

Roughan, M., Mace, A. J., Largier, J. L., Morgan, S. G., and Fisher, J. L. (2005a). Sub-surface recirculation and larval retention in the lee of a small headland: a variation on the upwelling shadow theme. *J. Geophys. Res.* 110:C10027. doi: 10.1029/2005JC002898

Roughan, M., and Middleton, J. H. (2002). A comparison of observed upwelling mechanisms off the east coast of Australia. *Cont. Shelf Res.* 22, 2551–2572. doi: 10.1016/S0278-4343(02)00101-2

Roughan, M., and Middleton, J. H. (2004). On the East Australian Current: variability, encroachment, and upwelling. *J. Geophys. Res.* 109, 1–16. doi: 10.1029/2003JC001833

Roughan, M., Oke, P. R., and Middleton, J. H. (2003). A modelling study of the climatological current field and the trajectories of upwelled particles in the East Australian Current. *J. Phys. Oceanogr.* 33, 2551–2564. doi: 10.1175/1520-0485(2003)033andlt;2551:AMSOTCandgt;2.0.CO;2

Roughan, M., Schaeffer, A., and Kioroglou, S. (2013). "Assessing the design of the NSW-IMOS moored observation array from 2008-2013: recommendations for the future," in *Oceans* (San Diego, CA), 1–7.

Roughan, M., Schaeffer, A., and Suthers, I. M. (2015). "Chapter 6-Sustained Ocean observing along the coast of southeastern Australia: NSW-IMOS 2007-2014," in *Coastal Ocean Observing Systems*, eds Y. Liu, H. Kerkering, and R. H. Weisberg (Boston, MA: Academic Press), 76–98.

Roughan, M., Terrill, E. J., Largier, J. L., and Otero, M. P. (2005b). Observations of divergence and upwelling around Point Loma, California. *J. Geophys. Res. Oceans* 110:C4. doi: 10.1029/2004JC002662

Schaeffer, A., Roughan, M., Austin, T., Everett, J. D., Griffin, D., Hollings, B., et al. (2016a). Mean hydrography on the continental shelf from 26 repeat glider deployments along Southeastern Australia. *Sci. Data* 3:160070. doi: 10.1038/sdata.2016.70

Schaeffer, A., Roughan, M., Jones, E., and White, D. (2016b). Physical and biogeochemical spatial scales of variability in the East Australian Current separation from shelf glider measurements. *Biogeosciences* 13, 1967–1975. doi: 10.5194/bgd-12-20101-2015

Schaeffer, A., Roughan, M., and Wood, J. E. (2014). Observed bottom boundary layer transport and uplift on the continental shelf adjacent to a Western Boundary Current. *J. Geophys. Res. Oceans* 119, 4922–4939. doi: 10.1002/2013JC009735

Truong, L., Suthers, I. M., Cruz, D. O., and Smith, J. A. (2017). Plankton supports the majority of fish biomass on temperate rocky reefs. *Mar. Biol.* 164, 73. doi: 10.1007/s00227-017-3101-5

van Sebille, E., Griffies, S. M., Abernathey, R., Adams, T. P., Berloff, P., Biastoch, A., et al. (2018). Lagrangian ocean analysis: fundamentals and practices. *Ocean Model.* 121, 49–75. doi: 10.1016/j.ocemod.2017.11.008

Wood, J. E., Schaeffer, A., Roughan, M., and Tate, P. M. (2016). Seasonal variability in the continental shelf waters off southeastern Australia: fact or fiction? *Cont. Shelf Res.* 112, 92–103. doi: 10.1016/j.csr.2015.11.006

Conflict of Interest: The authors declare that the research was conducted in the absence of any commercial or financial relationships that could be construed as a potential conflict of interest.